Improved performance of InGaN/GaN flip-chip light-emitting diodes through the use of robust Ni/Ag/TiW mirror contacts

Namig Hasanov, Binbin Zhu, Vijay Kumar Sharma, Shunpeng Lu, Yiping Zhang, Wei Liu, Swee Tiam Tan, Xiao Wei Sun, and Hilmi Volkan Demir

---

Articles you may be interested in

Formation process of high reflective Ni∕Ag∕Au Ohmic contact for GaN flip-chip light-emitting diodes
Appl. Phys. Lett. **90**, 163515 (2007); 10.1063/1.2730734

Investigation of Cr- and Al-based metals for the reflector and Ohmic contact on n - Ga N in GaN flip-chip light-emitting diodes
Appl. Phys. Lett. **89**, 191122 (2006); 10.1063/1.2387888

Theoretical demonstration of enhancement of light extraction of flip-chip GaN light-emitting diodes with photonic crystals
Appl. Phys. Lett. **89**, 091116 (2006); 10.1063/1.2338773

Cu -doped indium oxide∕Ag ohmic contacts for high-power flip-chip light-emitting diodes
Appl. Phys. Lett. **86**, 062103 (2005); 10.1063/1.1861494

Optical cavity effects in InGaN/GaN quantum-well-heterostructure flip-chip light-emitting diodes
Appl. Phys. Lett. **82**, 2221 (2003); 10.1063/1.1566098

Improved performance of InGaN/GaN flip-chip light-emitting diodes through the use of robust Ni/Ag/TiW mirror contacts

Namig Hasanov,[a] Binbin Zhu, Vijay Kumar Sharma, Shunpeng Lu, Yiping Zhang, Wei Liu, Swee Tiam Tan, Xiao Wei Sun, and Hilmi Volkan Demir
Luminous! Centre of Excellence for Lighting and Displays, Nanyang Technological University, 50 Nanyang Avenue S1-b3b-23, Singapore 639785

In this work, the authors report the incorporation of TiW alloy in InGaN/GaN-based flip-chip light-emitting diodes (LEDs). The advantages provided by the use of TiW are analyzed in detail. InGaN/GaN multiple quantum well LEDs with a Ni/Ag/TiW metal stack are found to tolerate high-temperature annealing better than those with a Ni/Ag metal stack. Highly improved current–voltage characteristics and enhanced optical output power are achieved for the devices with a TiW thin layer. These changes are ascribed to the higher reflectivity, smoother surface, and better ohmic properties of the device containing TiW after annealing. Better heat management of the device with TiW is demonstrated by comparing electroluminescence spectra of the two device structures. Overall, these factors resulted in devices with TiW exhibiting a higher external quantum efficiency than devices without TiW. Detailed x-ray photoelectron spectroscopy analyses of the reflector metal stacks reveal little intermixing of the layers after annealing in the devices with TiW. The results show that incorporation of TiW is a promising approach for the fabrication of high-performance InGaN/GaN flip-chip LEDs. © 2015 American Vacuum Society.
[http://dx.doi.org/10.1116/1.4939186]

I. INTRODUCTION

Fueled by enormous commercial interest, GaN-based light-emitting diodes (LEDs) have attracted great attention for a wide range of applications.[1,2] To achieve a high-quality LED, its external quantum efficiency (EQE) needs to be at the desired level. The EQE of a device depends on its internal quantum efficiency (IQE) and light extraction efficiency (LEE). Since the invention of LEDs, much effort has been devoted to improving IQE and LEE. The enhancement of IQE has been generally realized by tailoring the epitaxial structure,[3–7] or incorporation of plasmonic nanostructures.[8–10] Meanwhile, LEE can be improved by patterning the substrate,[11,12] using epitaxial structure[13,14] or current spreading layers,[15,16] fabricating different LED configurations (conventional, flip-chip or vertical), or including photonic crystals.[17–19]

Flip-chip LEDs (FCLEDs) possess a suitable configuration for high-power devices because of their effectiveness at increasing LEE and heat dissipation.[20] One of the major challenges to achieve high-performance FCLEDs is developing a high-quality metal stack with high reflectance and thermal conductivity that can serve as an efficient reflector with low forward voltage. Silver (Ag) has been widely used as a reflector layer in FCLEDs because of its high reflectivity and suitable electrical properties.[21–23] The poor adhesion of Ag directly onto a p-GaN surface leads to the degradation of both optical and electrical device performance.[24] A good solution to this problem is the introduction of a thin transparent layer between the p-GaN and Ag layers. Using this method, the adhesion between the reflector and GaN surface can be effectively improved, and the agglomeration of Ag can be alleviated to some extent. Oxidized nickel (Ni)[25,26] and indium tin oxide[27,28] have been widely used for this purpose. Although annealing can be used to improve current–voltage (I-V) characteristics, the quality of the Ag layer is still degraded by annealing. For example, previous studies have reported a large gap of around 15%–20% between the reflectivity levels of the as-deposited and annealed samples.[29,30] The degradation of the quality of the Ag reflector by high-temperature processing generally leads to a lower optical output power. Various attempts to address the issue of Ag agglomeration, such as having a Pt capping layer on AgCu alloy,[31] depositing a thin Ni cladding layer (2 nm) on top of a Ni/Ag reflector,[32] and testing AgAl alloy,[33] have been reported, but success was limited.

This work investigates the performance enhancement obtained by introducing a titanium tungsten (TiW) alloy layer on top of a Ni/Ag metal stack. The advantageous properties of W in this approach are its low electrical resistivity $(5.38 \times 10^{-8}\ \Omega\ \text{m})$ and high thermal conductivity (173 W/m K), as well as its effectiveness as a potential diffusion barrier for Ag.[34] The reflectance of the device with TiW is not decreased as much as that of the device without a TiW layer after annealing. The smaller red shift of electroluminescence (EL) of the device with TiW compared with that of the reference structure lacking TiW reveals that the former is better at heat management than the latter. Overall, these improvements of electrical and optical behavior give rise to an increase in EQE of 29% at 350 mA. This indicates that Ni/Ag/TiW can be used as an efficient metal stack for high-power FCLEDs.

II. EXPERIMENTAL SECTION

To investigate the properties of a Ni/Ag/TiW metal stack on a p-GaN surface, GaN LEDs were fabricated by

---

[a]Electronic mail: namig@ntu.edu.sg

metal–organic chemical vapor deposition (MOCVD) on a polar c-plane (0001) sapphire substrate.[35] A thin GaN nucleation layer (30 nm) was grown at low temperature before growth of a 2-μm layer of undoped-GaN (u-GaN). A 4 μm-thick n-doped GaN layer was deposited on top of u-GaN. The next step was the deposition of a multiple-quantum well (MQW) structure with five periods of InGaN/GaN, in which the well and barrier thicknesses were 3 and 10 nm, respectively. The last two steps were the fabrication of an electron blocking layer (20 nm p-doped AlGaN) and p-doped GaN layer (200 nm). The peak emission wavelength of the epitaxial LEDs was 452 nm with a full width at half-maximum of 24 nm [Fig. 1(a)]. Mg doped in the p-GaN layer was activated by high-temperature annealing in the MOCVD chamber. The measured concentration of holes after the activation was 3×10^{17} cm^{-3}, which is 1% of the overall dopant concentration.[36]

A schematic diagram of the structure of the fabricated device is presented in Fig. 1(b). For the electrodes, mesa patterns were formed by reactive ion etching using Cl$_2$ (20 sccm) and BCl$_3$ (40 sccm) gases. Ni (0.3 nm), Ag (200 nm), and TiW alloy (20 nm) layers were then deposited on top of the p-GaN surface by sputtering. The alloy was sputtered with 5% Ti and 95% W. The small amount of Ti helps to improve the adhesion between Ag and W. For comparison, a separate Ni/Ag reflector without TiW alloy was also deposited on a p-GaN surface. Finally, n- and p-type contact pads were deposited by electron beam evaporation. A high temperature annealing was performed to achieve ohmic contacts
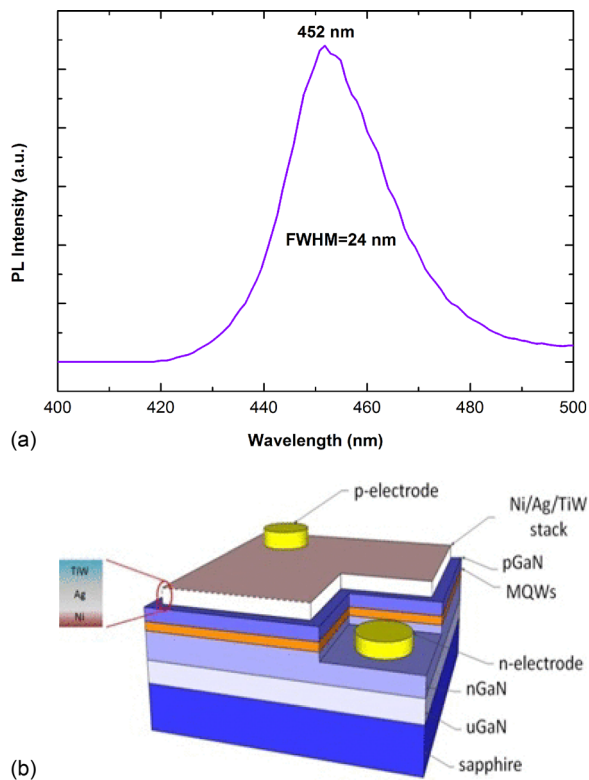
to the p-GaN layers. Annealing process shifts the surface Fermi level toward the valence band edge, which in turn reduces the band bending and the Schottky barrier height. Jipelec rapid thermal processing system was used to anneal the samples. The samples were annealed at 450 °C for 5 min in 500 sccm O$_2$ ambient. Annealing the reflector layers not only helps to achieve good ohmic contacts, it also oxidizes the thin Ni layer to make them transparent. Optical, electrical, and morphological properties of the devices with and without a TiW alloy layer were investigated. I-V characteristics of the fabricated devices were measured using a LED quick tester (M2442S-9 A, Quatek Group), and their optical reflectance was characterized by a UV-vis spectrometer. Surface morphology was examined with a LEO-1550 field-emission scanning electron microscope (FESEM). X-ray photoelectron spectroscopy (XPS) measurements were conducted using a 1486.7-eV Al Kα source. PL was measured with a spectrometer (RPM 2000, Nanometrics) using a He-Cd laser with an excitation wavelength of 325 nm as the excitation source. Optical power and EL characteristics were measured by an integrating sphere attached to a spectrometer (QE65000, Ocean Optics).

III. RESULTS AND DISCUSSION

Figure 2 presents FESEM images of the metal stacks with and without TiW after annealing at 450 °C. The as-deposited samples with and without TiW layers possess smooth surfaces. After annealing, the surface of the reference sample without TiW is rough [Fig. 2(b)]. In contrast, the sample with a TiW layer retains its smooth surface [Fig. 2(a)]. The smooth surface morphology of the device with TiW is attributed to TiW suppressing Ag agglomeration during annealing.

The higher quality of the contact mirror with TiW than that without TiW can also be observed in the insets of Fig. 2, which display emission images for the LEDs containing both types of reflectors. The Ni/Ag metal stack exhibits serious leakage of the emitted light [inset of Fig. 2(b)]. Conversely, the stack with TiW serves as a much better contact mirror, displaying uniform emission [inset of Fig. 2(a)], which is quantified next.

Figures 3(a) and 3(b) present the I-V and I–optical power characteristics of LEDs with a Ni/Ag/TiW alloy stack reflector and reference Ni/Ag reflector. The LED containing TiW annealed at 450 °C in O$_2$ (500 sccm) exhibits a forward voltage of 2.72 V at an injection current of 20 mA and reaches 3.09 V at 350 mA. In comparison, the forward voltage of the device without the TiW layer is 3.08 V at 20 mA and 3.48 V at 350 mA. The optical power of the device with TiW at low current (20 mA) is 20.26 mW. This device exhibits an output power of 298.78 mW at 350 mA. Meanwhile, the optical power of the reference device is 12.91 mW at 20 mA and 232.94 mW at 350 mA. The smaller heating droop of the device containing TiW with lower contact resistance and forward voltage compared with those of the reference one partly accounts for the substantial improvement of its optical output power.

FIG. 1. (Color online) (a) Photoluminescence (PL) spectrum of the LED epistructure. (b) Structure of the InGaN/GaN MQW FCLED with a Ni/Ag/TiW contact stack.
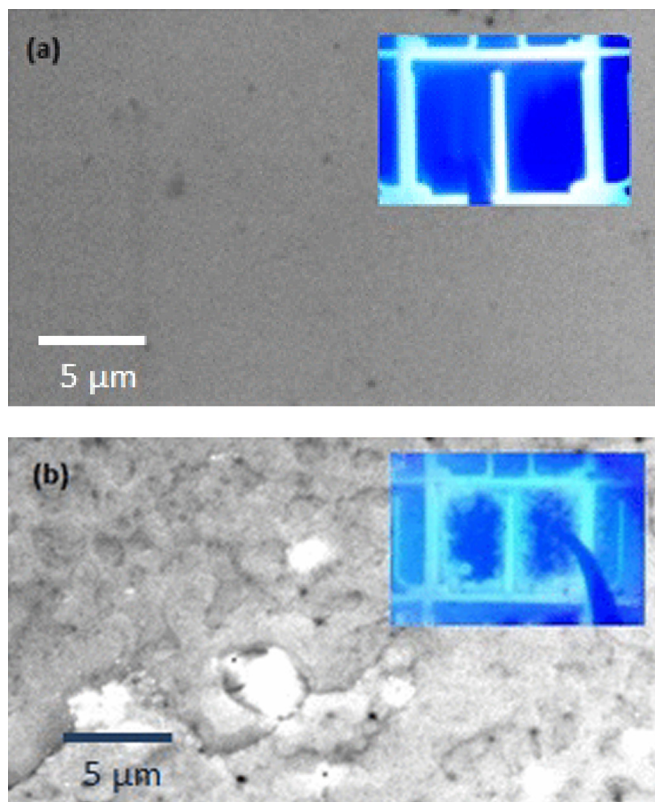
FIG. 2. (Color online) FESEM images of device surfaces with (a) Ni/Ag/TiW alloy stack and (b) Ni/Ag after annealing. Insets show emission from LEDs fabricated with the corresponding reflectors.

FIG. 3. (Color online) (a) Current–voltage and (b) current–power behavior of LED chips with and without TiW alloy.

To determine the effect of device heating on the optical performance of the structures, we measured EL intensities of both devices. The EL spectra for the TiW-containing and reference devices are depicted in Fig. 4. At 20 mA, both devices exhibited nearly the same EL peak wavelength (443 nm) (data not shown). The blue shift of 9 nm compared with the EL peak wavelength of the as-grown structure is attributed to self-screening of polarization induced by the quantum-confined Stark effect. However, when the current was increased to 150 mA, the EL peaks red-shifted, which is attributed to heating. At 150 mA, the device with the TiW alloy exhibited a smaller red shift (2.2 nm) than that of the reference device (4.5 nm). The smaller red shift arising from the better heat management in the device with TiW than in that without TiW is ascribed to the high thermal conductivity of the TiW alloy.

The high optical quality of the device with TiW retained after annealing also contributes to the observed improvement of optical output power, which is rationalized as follows. Figure 5 shows the reflectance spectra for devices with Ni/Ag/TiW and Ni/Ag metal stacks before and after annealing. Before annealing, almost the same reflectance curves were observed for both devices. After annealing, the device with the Ni/Ag/TiW reflector exhibits higher reflectance at 452 nm (88%) than that of the device with a Ni/Ag reflector (80%). For the device with the TiW alloy, the reflectance spectrum above 550 nm is approximately the same before and after annealing. However, there is a continuous gap
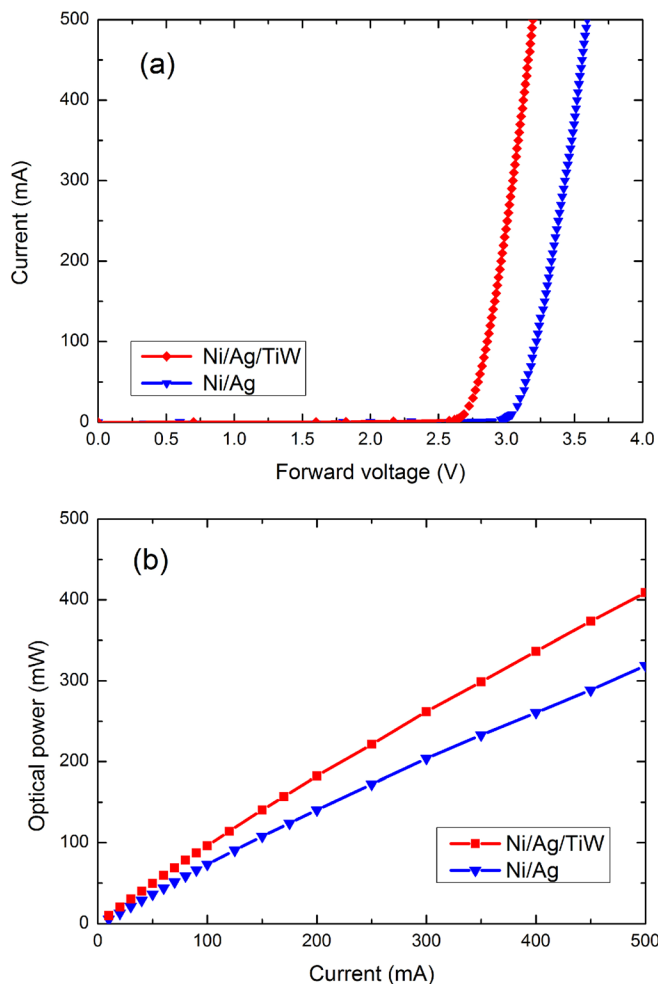
between the spectra of the reference device before and after annealing. The higher reflectivity of the device with a Ni/Ag/TiW reflector after annealing compared with that of the annealed reference device is attributed to TiW maintaining the uniformity of the main reflector film (Ag) during
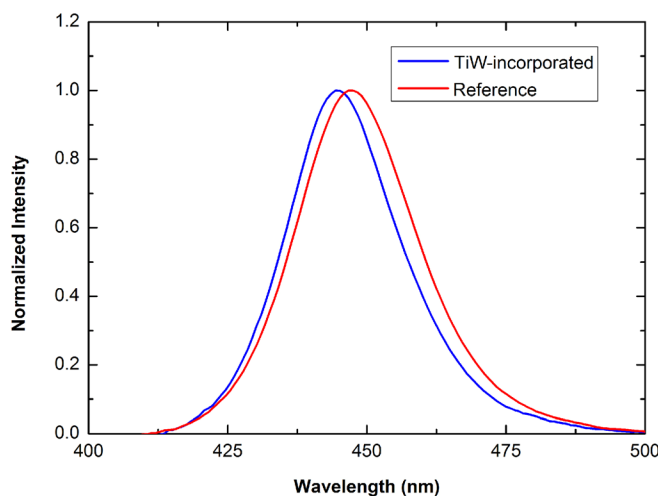

FIG. 4. (Color online) Normalized EL intensities of TiW-containing and reference devices at 150 mA.
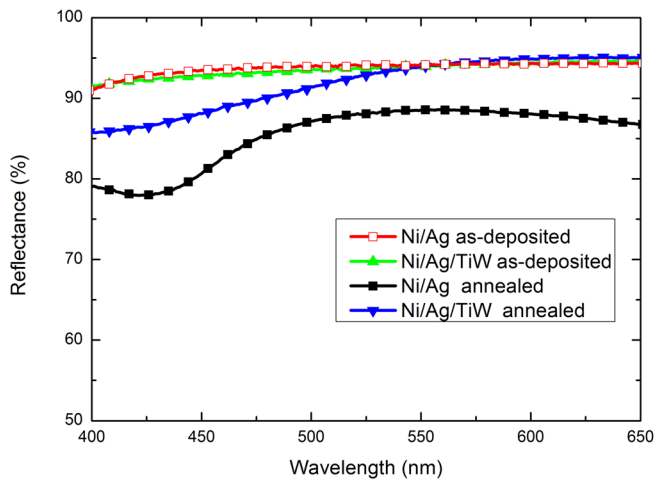
FIG. 5. (Color online) Reflectance spectra of devices with Ni/Ag/TiW and Ni/Ag reflectors before and after annealing.

FIG. 6. (Color online) Experimentally measured EQE as a function of current for devices with and without TiW.

annealing. The TiW layer protects Ag from aggregation and loss during high-temperature processing in O_2. Because W makes an excellent diffusion barrier for Ag, it can prevent or suppress Ag out-diffusion and thus maintain the quality of the Ag layer during high-temperature annealing. Therefore, the reflectivity of the Ni/Ag/TiW metal stack can be retained after annealing compared with that of the Ni/Ag metal stack.

EQE measurements for devices with and without TiW following annealing are presented in Fig. 6. The presence of TiW increases the maximum EQE of the devices from 26% to 36%. The EQE values for the reference and TiW-containing devices at 350 mA are 24% and 31%, respectively. The considerable enhancement of EQE is attributed to the better light extraction and thermal management, and lower contact resistance and forward voltage of the structure with a thin layer of TiW alloy.
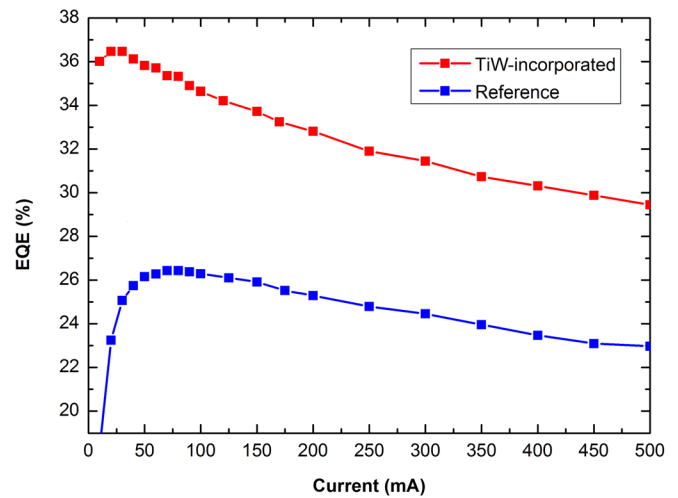
Figures 7(a) and 7(b) present the survey spectra for the surface of the device with a Ni/Ag/TiW metal stack in the range of 10–1350 eV before and after annealing, respectively. The detected materials are W, Ti, and O in both cases. The $4d_{5/2}$, $4d_{3/2}$, and $4f_{7/2}$ peaks of W were detected with higher intensities. Because annealing was performed in O_2, there is a visible increase in the intensity of the O 1s peak after annealing. Ag could not be detected on the top surface after high-temperature processing. Therefore, TiW has successfully prevented the out-diffusion of Ag during high-temperature processing.

Figure 8 displays XPS depth profile measurements obtained to examine the interfacial reactions within Ni/Ag/TiW and between the metal stack and p-GaN. Before annealing [Fig. 8(a)], O_2 is only observed on the outermost layer.
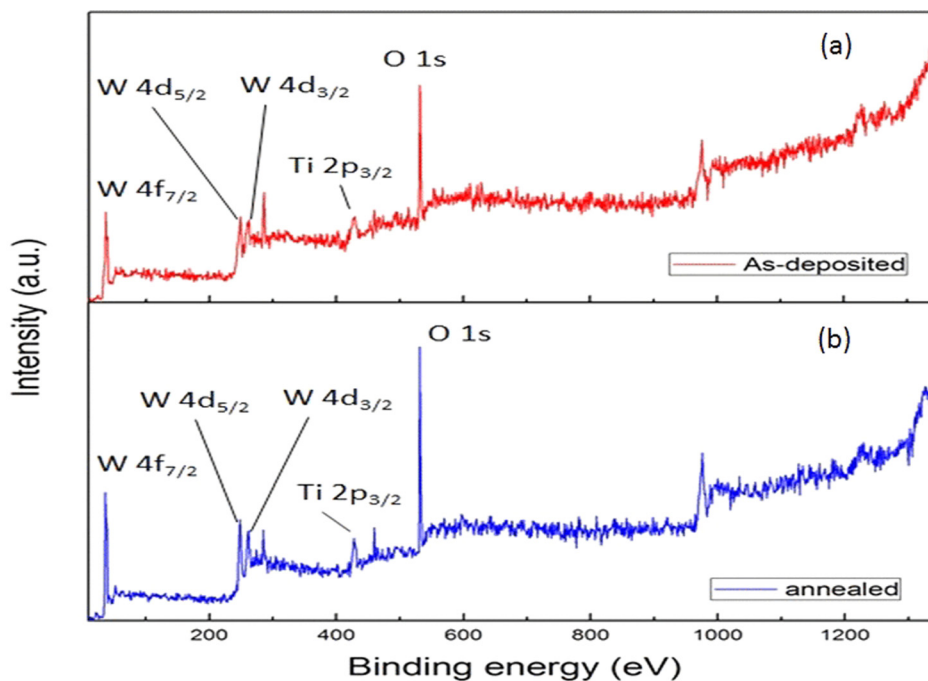

FIG. 7. (Color online) Survey spectra of the surface of the device with a Ni/Ag/TiW alloy stack reflector (a) before and (b) after annealing.
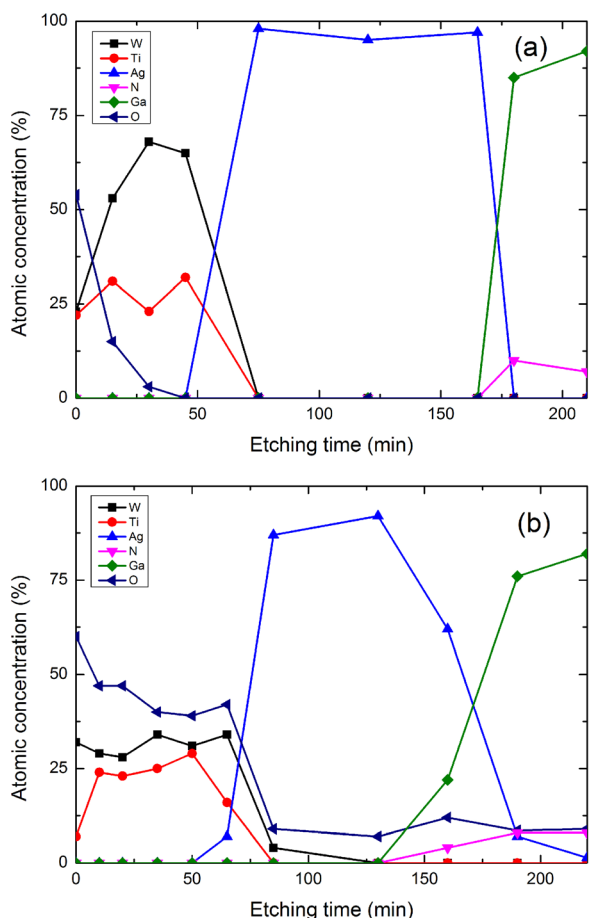
FIG. 8. (Color online) XPS depth profiles of the Ni/Ag/TiW contact mirror on p-GaN (a) before and (b) after annealing.

However, after annealing [Fig. 8(b)], O_2 diffusion to the Ag/p-GaN interface was observed. The diffusion of O_2 to the Ag/p-GaN interface is critical for the formation of NiO, which enables a good ohmic contact to be realized. Figure 8(b) reveals that the out-diffusion of Ag through TiW is negligible, thus showing the effectiveness of TiW as an Ag diffusion barrier layer. TiW preserves the Ag layer during annealing so that the Ag layer retains high reflectivity. However, there is interdiffusion of Ag and Ga at the Ag/p-GaN interface. The in-diffusion of Ag into p-GaN could be the reason for the slight decrease in the reflectivity of the Ni/Ag/TiW reflector at 452 nm following annealing, as shown in Fig. 6. This will be further addressed in our future work. Meanwhile, the out-diffusion of Ga atoms leaves a large number of Ga vacancies at the Ag/p-GaN interface, which can benefit the formation of an ohmic contact. Because the Ni layer was only 0.3 nm thick to achieve better adhesion of Ag and p-GaN, the signal for this thin layer could not be detected. The XPS analyses readily explain the mechanisms behind the considerable improvement of the electrical and optical properties of the flip-chip device with TiW alloy. These improvements include the higher optical output power and EQE of the LED with a Ni/Ag/TiW reflector than those of the one with a Ni/Ag reflector.

IV. SUMMARY AND CONCLUSIONS

In summary, the effects of TiW alloy on the performance of InGaN/GaN MQW FCLEDs were systematically investigated. The TiW alloy layer effectively limits Ag agglomeration during annealing. Unlike the reference structure, the Ni/Ag/TiW metal stack was optically stable after annealing at 450 °C. The reflectance of the TiW-containing LED was 88% at 452 nm, considerably higher than that of the reference structure without TiW alloy (80%). FCLEDs with a Ni/Ag/TiW reflector annealed at 450 °C exhibited an optical power of 298.78 mW at 350 mA, which was 28% higher than the output power of the reference device at the same current. The smaller red shift of EL upon annealing compared with that of the reference device revealed the better heat management capability of the TiW-containing device. In addition, EQE was substantially enhanced by the introduction of the thin alloy layer. These results reveal that a TiW alloy layer can improve the performance of GaN-based MQW FCLEDs.

ACKNOWLEDGMENTS

[1]H. Morkoç, S. Strite, G. B. Gao, M. E. Lin, B. Sverdlov, and M. Burns, J. Appl. Phys. **76**, 1363 (1994).
[2]H. X. Jiang, S. X. Jin, J. Li, J. Shakya, and J. Y. Lin, Appl. Phys. Lett. **78**, 1303 (2001).
[3]Z.-H. Zhang *et al.*, Opt. Express **21**, 4958 (2013).
[4]Z. Kyaw *et al.*, Opt. Express **22**, 809 (2014).
[5]Z. Zhang, S. T. Tan, J. Zhengang, L. Wei, J. Yun, Z. Kyaw, Y. Dikme, S. X. Wei, and H. V. Demir, J. Display Technol. **9**, 226 (2013).
[6]Z.-H. Zhang *et al.*, Opt. Lett. **39**, 2483 (2014).
[7]Z. G. Ju *et al.*, ACS Photonics **1**, 377 (2014).
[8]C.-Y. Cho, K. S. Kim, S.-J. Lee, M.-K. Kwon, H. Ko, S.-T. Kim, G.-Y. Jung, and S.-J. Park, Appl. Phys. Lett. **99**, 041107 (2011).
[9]Y. Li *et al.*, J. Appl. Phys. **114**, 113104 (2013).
[10]C.-Y. Cho, Y. Zhang, E. Cicek, B. Rahnema, Y. Bai, R. McClintock, and M. Razeghi, Appl. Phys. Lett. **102**, 211110 (2013).
[11]H. Y. Lin, Y. J. Chen, C. C. Chang, X. F. Li, S. C. Hsu, and C. Y. Liu, Electrochem. Solid-State Lett. **15**, H72 (2011).
[12]H.-Y. Wang, Z.-T. Lin, J.-L. Han, L.-Y. Zhong, and G.-Q. Li, Chin. Phys. B **24**, 067103 (2015).
[13]Z. Zuo, D. Liu, B. Zhang, J. He, H. Liu, and X. Xu, Phys. Status Solidi A **208**, 2226 (2011).
[14]T. S. Kim, S.-M. Kim, Y. H. Jang, and G. Y. Jung, Appl. Phys. Lett. **91**, 171114 (2007).
[15]D. Tao, Z. Bei, K. X. Ning, B. Kui, Z. W. Zhu, D. S. Xu, Z. G. Yi, and G. Z. Zhao, IEEE Photonics Technol. Lett. **20**, 1974 (2008).
[16]J. Q. Xi, H. Luo, A. J. Pasquale, K.-S. Kim, and E. F. Schubert, IEEE Photonics Technol. Lett. **18**, 2347 (2006).
[17]M. Elison and W. Claude, J. Phys. D: Appl. Phys. **43**, 354005 (2010).
[18]P.-H. Fu, G.-J. Lin, H.-P. Wang, K.-Y. Lai, and J.-H. He, Nano Energy **8**, 78 (2014).
[19]G. M. Wu, B. H. Tsai, S. F. Kung, and C. F. Wu, Acta Phys. Pol. **120**, 140 (2011).
[20]W. S. Chen *et al.*, IEEE Trans. Electron Device **53**, 32 (2006).
[21]J. O. Song, J. S. Kwak, Y. Park, and T. Y. Seong, Appl. Phys. Lett. **86**, 062104 (2005).
[22]S.-H. Park, J.-W. Jeon, and T.-Y. Seong, J. Korean Phys. Soc. **59**, 156 (2011).
[23]H. W. Jang and J.-L. Lee, Appl. Phys. Lett. **85**, 5920 (2004).

24Y. T. Hwang, H. G. Hong, T. Y. Seong, D. S. Leem, T. Lee, K. K. Kim, and J. O. Song, Mater. Sci. Semicond. Process. **10**, 14 (2007).

25H. J. Song, C. H. Roha, H. G. Choi, M.-W. Ha, C.-K. Hahna, J. H. Park, and J. H. Lee, Appl. Surf. Sci. **257**, 8102 (2011).

26F. Jiang, L.-E. Cai, J.-Y. Zhang, and B.-P. Zhang, Physica E **42**, 2420 (2010).

27T. Jeong, S. H. Lee, H. H. Lee, S. H. Jeong, J. G. Jhin, and J. H. Baek, J. Korean Phys. Soc. **55**, 1615 (2009).

28S. Kim, J.-H. Jang, and J.-S. Lee, J. Electrochem. Soc. **154**, H973 (2007).

29J.-S. Park, J. Han, J.-W. Han, H. Seo, J.-T. Oh, and T.-Y. Seong, Superlattice Microstruct. **64**, 7 (2013).

30W.-S. Yum, J.-W. Jeon, J.-S. Sung, and T.-Y. Seong, Opt. Express **20**, 19194 (2012).

31S. H. Kim, T. H. Kim, J. W. Bae, and G. Y. Yeom, Thin Solid Films **521**, 54 (2012).

32J. H. Son, Y. H. Song, H. K. Yu, and J.-L. Lee, Appl. Phys. Lett. **95**, 062108 (2009).

33J.-Y. Kim *et al.*, Appl. Phys. Lett. **88**, 043507 (2006).

34S. Bhagata, H. Hanb, and T. L. Alforda, Thin Solid Films **515**, 1998 (2006).

35Z. Zhang *et al.*, Opt. Express **22**, 779 (2014).

36H. Tokunaga, A. Ubukata, Y. Yano, A. Yamaguchi, N. Akutsu, T. Yamasaki, and K. Matsumoto, J. Cryst. Growth **272**, 348 (2004).